

Multispectral imaging of healthy and diseased red blood cells using confocal microscopy

Laura Rey-Barroso^{a*}, Mónica Roldán^{be},
Francisco J. Burgos-Fernández^a, Ignacio Isola^{ce},
Anna Ruiz-Llobet^d, Susanna Gassiot^{cd}, Meritxell Vilaseca^a

^aCentre for Sensors, Instruments and Systems Development, Technical University of Catalonia, Terrassa, Spain

^bUnit of Confocal Microscopy, Service of Pathological Anatomy, Pediatric Institute of Rare Diseases, Hospital Sant Joan de Déu, Esplugues de Llobregat, Spain

^cLaboratory of Hematology, Service of Laboratory Diagnosis, Hospital Sant Joan de Déu, Esplugues de Llobregat, Spain

^dService of Pediatric Hematology, Hospital Sant Joan de Déu, Esplugues de Llobregat, Spain

^eInstitute of Pediatric Research, Hospital Sant Joan de Déu, Esplugues de Llobregat, Spain

*Corresponding author: laura.rey.barroso@upc.edu

Presenting author: Laura Rey-Barroso

ABSTRACT

Red blood cell disorders represent the most common single-gene defects and pose a major public health problem, particularly in tropical countries, occurring with high frequency. Their diagnose can sometimes be difficult due to the coexistence of different causes of anemia, such as thalassemia and iron deficiency, and blood transfusions, among other factors, and requires expensive and complex molecular tests. In this work, blood samples from patients with different syndromes of alpha-thalassemia and iron deficiency (including anemia) as well as healthy (control) subjects were analyzed under a Leica TCS SP8 confocal microscope. Samples exhibited autofluorescence when excited at 405 nm and three experimental descriptors calculated from the mean emission intensities at 502 nm, 579 nm, 628 nm, and 649 nm allowed us to discriminate between diseased and healthy cells. According to the results obtained, spectral confocal microscopy could serve as a tool in the diagnosis of thalassemia.

KEYWORDS

multispectral imaging | confocal microscopy | thalassemia | red blood cell | autofluorescence

INTRODUCTION

Red blood cells (RBCs) are specialized cells in charge of oxygen transportation throughout the body. They contain a tetramer called hemoglobin that is able to bind oxygen and carbon dioxide molecules. In thalassemia, hemoglobin is known to have alterations in the globin chains that form its quaternary structure. An unbalanced production of either one of the two globin chains (alpha or beta) produces a quantitative alteration in hemoglobin. This can cause very variable manifestations, from none in asymptomatic carriers, to serious abnormalities that include severe anemia, extramedullary hematopoiesis, skeletal and growth deficits and iron overload, with a significantly shortened life expectancy in the absence of treatment. According to Provan *et al.* (2015), the severity of the clinical features correlates with the number of functioning globin genes that are lost. Iron deficiency is the other major cause of microcytic anemia besides thalassemia, and this can be associated with a markedly abnormal RBC morphology. The diagnosis of thalassemia is based on RBC morphology under conventional optical microscopy and RBC indices. These techniques are sometimes not sufficiently specific enough to distinguish between mild forms of the disease, which show no symptoms or very mild ones and have similar RBC indices; additionally, thalassemia can also be confused with other causes of anemia such as iron deficiency.

Complex and expensive genetic studies are often required to diagnose individuals with this disease. For this reason, diverse studies have been conducted under experimental and commercial spectroscopic systems to establish reflectance, emission and/or absorption differences in the ultraviolet (UV), visible (VIS) and near infrared (NIR) ranges between healthy and unhealthy RBCs. Gunasekaran *et al.* (2008) proved that there are statistically significant optical density differences in the range from 200 to 700 nm between RBCs of patients with leukemia, anemia, liver cirrhosis, thalassemia and diabetes with respect to healthy individuals. Alsalhi *et al.* (2014) used a spectrofluorometer for the spectral detection of thalassemia and observed two peaks at 580 nm and 630 nm, mostly due to the basic and neutral forms of porphyrin, a type of nitrogenous biological pigment that forms the heme group. Nevertheless, in all of the aforementioned studies, the spectral differences that may underlie different clinical presentations of thalassemia (especially mild forms) were not reported. This might have been due to a lack of spectral differences, or because the integrated spectroscopic information provided was not spatially accurate enough to reveal such differences.

The use of spectral imaging improves RBC analysis since it adds spatial resolution to spectroscopic data. Dai *et al.* (2013) used a molecular hyperspectral imaging system to identify blood cells. This system was developed according to a push-broom approach covering the 400–860 nm range; spectral pattern traits were obtained from the background, red cells, lymphocytes, nuclei, and plasma of tumor cells. Kurtuldu *et al.* (2018) developed a hyperspectral microscope based on a liquid crystal tunable filter to detect by image classification the different elements in a RBC from 420 nm to 730 nm. Other authors have analyzed RBCs under confocal microscopy, which, unlike traditional microscopy, allows the sample to be scanned at different depths obtaining axial cuts of the sample with autofluorescence or reflectance information. Reflectance confocal microscopy (RCM) has been demonstrated to be useful for obtaining information about the physiological properties of RBCs at high resolution and without the need for fluorescence labeling according to Golan and Yelin (2010) and Zeidan and Yelin (2015). Khairy *et al.* (2008) obtained tridimensional (3D) confocal microscope images of RBCs labeled with fluorescent dyes and compared them to mathematical simulations of the shapes by means of spherical harmonic series expansions. Rappaz *et al.* (2008) compared the morphological values obtained from different imaging techniques, including confocal microscopy. In order to perform a volume assessment of RBCs under confocal laser scanning microscopy (CLSM), cells were labeled with a fluorescent dye and excited at 561 nm, and the emission was collected from 580 nm to 700 nm.

As can be inferred from the state-of-the-art, the use of spectral imaging techniques together with CLSM could provide spectroscopic information in 3D of the functional and metabolic state of the cell, collecting the reflectance, autofluorescence, or even fluorescence arising from the staining of different cellular components with the use of extrinsic fluorescent probes. The purpose of the present work is to analyze the spectral and morphological characteristics of healthy and diseased RBCs from pediatric patients with thalassemia, under a spectral confocal microscope, a powerful imaging instrument that has not yet exploited as a diagnostic tool for RBC diseases. In addition, blood samples from patients with iron deficiency are also studied and compared to thalassemia samples.

EXPERIMENTS

Blood samples from 17 pediatric patients between 1 and 17 years old were evaluated, including patients with different forms of alpha-thalassemia, patients with different degrees of iron deficiency and healthy individuals as controls. They were carefully loaded into container dishes, CELLview™ (Greiner Bio One GmbH, Courtaboeuf, France), which incorporate a cell-adhesion layer preventing the movement of cells during the measurements. For the living RBCs to remain under the same conditions as inside the human body, neither the addition of solvents, such as saline solution, nor the centrifugation of the sample to remove other cellular types and components in blood was considered. Samples were not labeled with extrinsic fluorescent probes to avoid overlying spectral information. Blood samples were collected in tubes containing lithium heparin, a frequently used anticoagulant agent to avoid sample corruption. RBC indices were analyzed using an ADVIA 2120i hematology analyzer (Siemens Healthcare Diagnostics Inc., Erlangen, Germany).

The study group consisted of eight healthy subjects, labeled TC1–TC8, including one patient with HbH alpha-thalassemia (homozygous for a HbA2 c.*93_*94delAA mutation), which is considered severe, labeled T1; a patient with alpha-thalassemia minor (Southeast Asian [SEA] heterozygous deletion), identified as T2; and four asymptomatic alpha-thalassemia carriers (3.7 kb heterozygous deletion), labeled T3–T6. In addition, the samples of the three patients suffering from different degrees of iron deficiency were analyzed and labeled TA1–TA3.

The samples were analyzed under a Leica TCS SP8 confocal microscope with stimulated emission depletion (STED) at 3x super resolution (Leica Microsystems GmbH, Mannheim, Germany), equipped with a detection unit of hybrid detectors capable of detecting signals arising from RBCs from 400 nm to 790 nm. It incorporates two lasers for excitation, a diode laser with an emission of 405 nm and a white laser that emits from 470 nm to 670 nm, combined with an acoustic-optic tunable filter (AOTF). To collect the spectral emission of RBCs produced by autofluorescence, a 63x (NA 1.4, oil) plan-apochromatic objective was used. The confocal microscope could focus at several depths within the volume of blood, where RBCs were clearly differentiated and displaced throughout the sample, acquiring several fields to evaluate emission uniformity. Samples were excited at 405 nm with a blue diode laser line and the AOTF was set at 65%. Emission images from 425 nm to 790 nm were acquired with a spectral window of 20 nm and in steps of 7 nm. The variation in intensity of a particular spectral component was represented on the screen using a pseudo-color look-up table.

RESULTS AND DISCUSSION

Figure 1 contains sequences of confocal emission images captured at different wavelengths for some samples when excited at 405 nm. For each sample, spectral emission images at 453 nm, 502 nm, 579 nm, 628 nm, and 649 nm of a given imaged field are included, as well as the average emission curves considering the cellular structures (RBCs, surrounded by a dashed white contour).

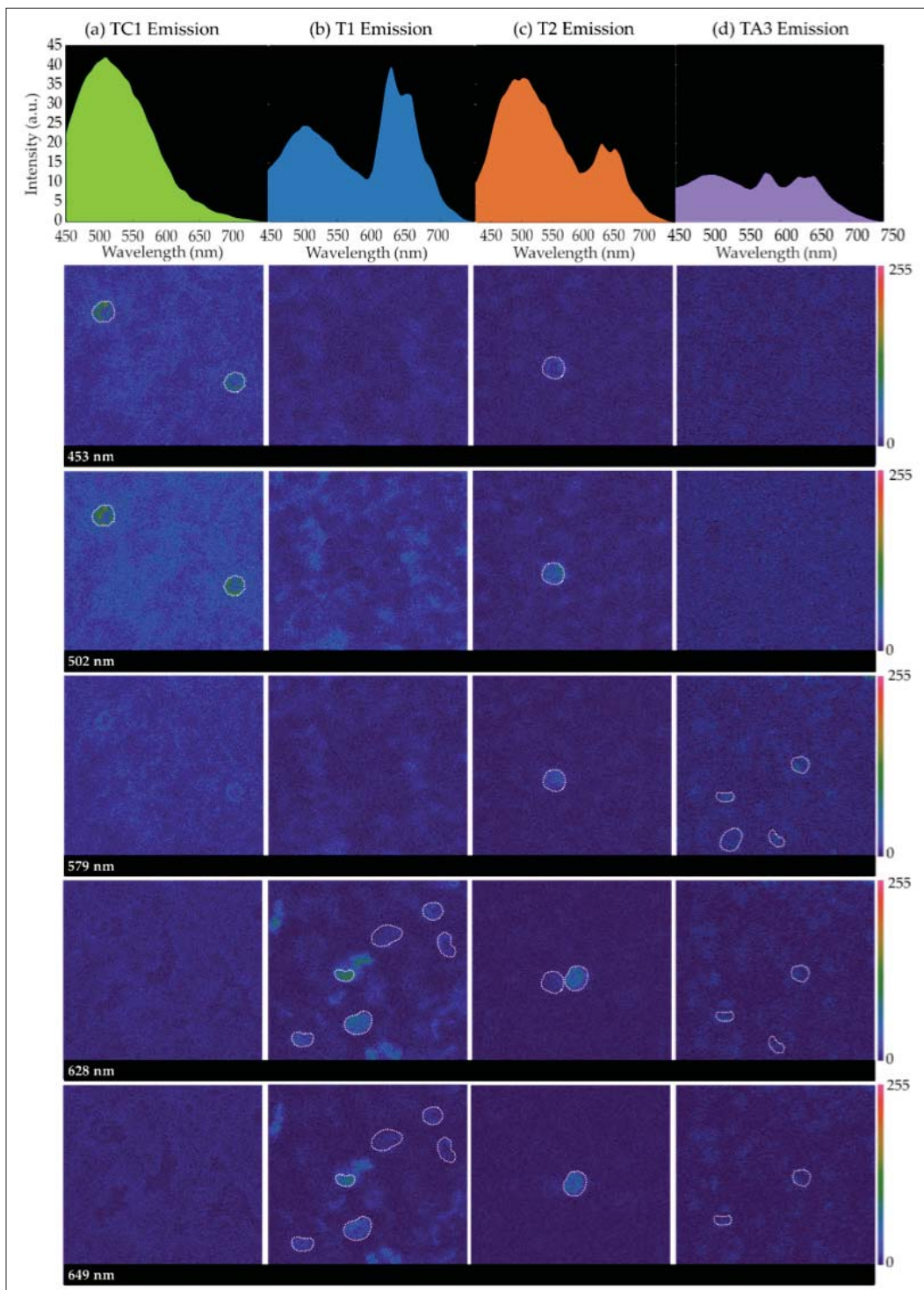


Figure 1: Intensity vs. wavelength (top) and images from autofluorescence RBCs (bottom) corresponding to 453 nm, 502 nm, 579 nm, 628 nm, and 649 nm wavelengths, for the following samples: (a) TC1, from a control patient; (b) T1, HbH (severe alpha-thalassemia); (c) T2, SEA heterozygous deletion (mild); (d) TA3 iron-deficiency anemia.

They all present a peak around 502 nm created by all sample emission, background and cellular structures. Paying attention to the spectral images collected at 579 nm, 628 nm and 649 nm, it can be inferred that, for samples corresponding to HbH disease (T1), SEA deletion (T2) and iron deficiency (TA3), some cellular structures appear brighter. Sometimes, one of the latter peaks of emission is greater than that at 502 nm (T1 and TA3). Emission images were captured for different areas of the samples where a sufficiently large number of RBCs were visible.

The populations of cells that were found to emit differently than the background were especially high in the samples of the diseased groups. In order to obtain a general overview of the emission, circular regions of 4 μm were sketched on top of one to 10 RBCs as regions of interest on every field using the Leica Application Suite X (LAS X) software (Leica Microsystems GmbH, Mannheim, Germany). Finally, T4 and TC2 were not included due to the insufficient number of evaluated fields for their analysis. Studies using the state-of-the-art approaches have obtained similar emission spectra for normal and diseased RBCs. Distinct and well-defined bands beyond 600 nm are generally attributed to porphyrins and a heme-altered metabolite. Liu *et al.* (2003) detected a peak around 628 nm produced in the emission curves of some samples, which was attributed to porphyrin. This compound is a nitrogenized biological pigment whose derivative products include hemoproteins, which are made of a combination of porphyrin, metals and proteins. Porphyrin provides RBCs with their characteristic red color. It is thought that the amount of free porphyrin in blood is greater in patients suffering from alpha-thalassemia and iron-deficiency anemia than in healthy individuals Meloni *et al.* (1982), which is consistent with the findings of our study.

CONCLUSIONS

The combination of CLSM with spectrofluorometry techniques is a powerful tool that allows the direct analysis of fluorescent pixels and their 3D location *ex-vivo* in the whole specimen, minimizing the artefacts associated with sample processing. Other techniques may allow the imaging of the specimen at specific depths from which the signal of interference arises, but they do not provide sufficient excitation wavelengths as well as spectral windows of detection to explore the different spectral traits in depth. Since thalassemia has unspecific imaging characteristics, of the few described state-of-the-art approaches that we tried to reproduce, the best tool to work with is confocal imaging and the super-resolution provided by the microscope used. The intensities measured at 502 nm, 628 nm and 649 nm when exciting RBCs at 405 nm allowed a discrimination between healthy and diseased individuals that presented with anemia (thalassemia or iron deficiency) and between different degrees of influence in alpha-thalassemia, with less accuracy due to the small sample size. The difference in fluorescence resulting from these parameters may reside in heme group degradation, which is associated to oxidative stress. Nagababu *et al.* (2008) have found heme degradation products in thalassemic mice, which share with humans the gene clones that might be affected in this and other hemoglobinopathies. In this case, authors excited samples with a 321 nm laser wavelength and obtained two fluorescent emission bands, with a predominant peak at 480 nm. It would have been interesting to excite our samples with shorter wavelengths than 405 nm without compromising the viability of the cells; however, with commercial confocal microscopes, this is the shortest wavelength available. In addition, the authors suggested that the cell membrane might be affected due to the release of iron from the heme group degradation, for instance, membrane skeletal spectrin according to Datta *et al.* (2003). An imbalance in the bilipid membrane affects the cytoadherence; thus, these diseased RBCs have difficulties circulating through certain vessels—for instance, the ones in the spleen, causing splenomegaly. It would be interesting to carry out another type of assay, referred to as the immuno-labeling of the cell membrane, which can only be carried out with the cells fixated; this would be helpful for detecting affectations in the structure of the cell membrane, which are not currently clearly determined. Nevertheless, another advantage of the combined use of the imaging techniques described in this work, is that it does not necessarily require reagents or the use of markers and fixating substances used to capture absorption spectra. Thus, tests can be carried out in normal physiological conditions without the need to prepare hemolyzed serums and with a relatively low volume of RBCs. Future work will consist of expanding the set of samples to corroborate the effectiveness of the ratios described. We will also need to corroborate the results by trying to reproduce the same experiments in a different hospital. Open source neural network models will be used to analyze our set of images in further detail, and thus we will obtain better screening results. The current and future research may offer hematologists with a new approach to improving diagnostic strategies and searching for involved genes.

ACKNOWLEDGEMENTS

We would like to thank the Spanish Ministry of Economy and Competitiveness, grant number DPI2017-89414-R.

REFERENCES

- Alsalhi, M.S., F.H. Algahtani, S. Devanesan, V.T. Vijmasi, K. Jeyaprakash, A.H. Alsaheed, and V. Masilamani.** 2014. Spectral detection of thalassemia: A preliminary study. *J. Biomed. Sci.* 21: 1–8.
- Dai, C., Q. Li and J. Liu.** 2013. Blood cells classification using hyperspectral imaging technique. *J. Bioinform. Biol. Eng.* 1: 27–33
- Datta, P., S.B. Chakrabarty, A. Chakrabarty, A. Chakrabarti.** 2003. Interaction of erythroid spectrin with hemoglobin variants: Implications in δ -thalassemia. *Blood Cells Mol. Dis.* 30: 248–253.
- Golan, L. and D. Yelin.** 2010. Flow cytometry using spectrally encoded confocal microscopy. *Opt. Lett.* 35: 2218.
- Gunasekaran, S., R.K. Natarajan, and V. Renganayaki.** 2008. UV visible spectrophotometric approach and absorption model for the discrimination of diseased blood. *Asian J. Chem.* 20: 48–54.
- Khairy, K., J. Foo, and J. Howard.** 2008. Shapes of Red Blood Cells: Comparison of 3D Confocal Images with the Bilayer-Couple Model. *Cell. Mol. Bioeng.* 1: 173–181.
- Kurtuldu, H., A.D. Oktan, H. Candan and B.S. Cihangiroglu.** 2018. Red Blood Cell Analysis by Hyperspectral Imaging. *Nat. Appl. Sci. J. 2*, 1: 9–15.
- Liu, K.Z., K.S. Tsang, C.K. Li, R.A. Shaw, and H.H. Mantsch.** 2003. Infrared spectroscopic identification of δ -thalassemia. *Clin. Chem.* 49: 1125–1132.
- Meloni, T., D. Gallisai, M. Demontis, and S. Erre.** 1982. Free erythrocyte porphyrin (FEP) in the diagnosis of δ -thalassaemia trait and iron deficiency anaemia. *Haematologica* 67: 341.
- Nagababu, E., M.E. Fabry, R.L. Nagel, and J.M. Rifkind.** 2008. Heme degradation and oxidative stress in murine models for hemoglobinopathies: Thalassemia, sickle cell disease and hemoglobin C disease. *Blood Cells Mol. Dis.* 41: 60–66.
- Provan, D., T. Baglin, I. Dokal, and J. de Vos.** 2015. *Oxford Handbook of Clinical Haematology*. Oxford: Oxford University Press.
- Rappaz, B., A. Barbul, Y. Emery, R. Korenstein, C. Depeursinge, P.J. Magistretti, and P. Marquet.** 2008. Comparative study of human erythrocytes by digital holographic microscopy, confocal microscopy, and impedance volume analyzer. *Cytom. Part A* 73: 895–903.
- Zeidan, A. and D. Yelin.** 2015. Reflectance confocal microscopy of red blood cells: Simulation and experiment. *Biomed. Opt. Express* 6: 4335.